

SWITCHING CONTROLLER FOR BUCK-BOOST CONVERTER WITH INVERTING TOPOLOGY

Valery D. Yurkevich

*Automation Department, Novosibirsk State Technical University
Novosibirsk, 630092, Russia, e-mail: yurkev@ac.cs.nstu.ru*

Abstract: The problem of output regulation with guaranteed transient performances for buck-boost converter with inverting topology is discussed. The fast dynamical controller with the relative highest derivative of output signal in feedback loop is used. Consequently, two-time-scale motions are induced in the closed-loop system. Stability conditions imposed on the fast and slow modes and sufficiently large mode separation rate can ensure that the full-order closed-loop system achieves the desired properties in such a way that the output transient performances are desired and insensitive to external disturbances and parameter variations in the system. The existence of stable limit cycle in the fast motion subsystem gives the robustness of the output transient performances in the presence of external disturbance and parameter uncertainty. *Copyright ©2005 IFAC*

Keywords: converters, proportional plus integral action controller, nonlinear control systems, output regulation, singular perturbation method.

1. INTRODUCTION

There is a broad set of references devoted to analysis and design of switching buck, boost, or buck-boost converters. In the most of references the derivation of the converter circuit topology is discussed really (Maksimovic and Cuk, 1991; Jianping Xu, 1991; Mohan *et al.*, 1995; Giral *et al.*, 2002; Bryant and Kazimierzuk, 2002), rather than methods of switching controller design.

The subject matter of this paper is the guaranteed cost control for buck-boost converter with inverting topology under uncertainties of parameters and external disturbances represented by varying value of a load resistance. Hence, optimization techniques can not be applied for the discussed control problem solution. As far as nonsmooth nonlinearities are inherent property of such power converters, then the control system design methodology based on sliding modes (Cunha and Pagano, 2002; Shtessel *et al.*, 2002; Sira-Ramirez,

2002) is widely used for this purpose in presence of uncertainties.

The control system with the highest derivative in feedback (Vostrikov, 1977) applied to a buck-boost converter is discussed in the paper as well as peculiarities caused by fast oscillations in such system. Note that the analysis of fast oscillations by the describing function method in the control systems with the highest derivative and differentiating filter in feedback was discussed in (Suvorov, 1991). In the recent paper the modified control law structure (Yurkevich, 2004) with the highest derivative of output signal in feedback loop is used and by that the integral action can be included in the control loop.

The paper is organized as follows. First, a model of the buck-boost converter with inverting topology is defined. Next, the discussed design method, influence of fast oscillations, and simulation results are presented.

2. BUCK-BOOST CONVERTER

2.1 Buck-boost converter with inverting topology

Let us consider the buck-boost converter with inverting topology, shown in Fig. 1. The switched

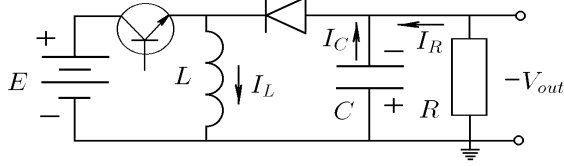


Fig. 1. Buck-boost converter circuit.

model of the buck-boost converter is given by

$$\dot{x}_1 = \frac{E}{L}u - \frac{x_2}{L}(1-u), \quad (1)$$

$$\dot{x}_2 = -\frac{1}{RC}x_2 + \frac{x_1}{C}(1-u), \quad (2)$$

where $x_1 = I_L$, $x_2 = V_C = V_{out}$ and u takes values in the set $\{0, 1\}$.

2.2 Buck-boost converter control task

The control problem is to provide the following condition:

$$\lim_{t \rightarrow \infty} V_C(t) = V_C^d \quad (3)$$

where V_C^d is the reference value (reference input) of voltage drop V_C across a capacitor. Moreover, the controlled transients $V_C(t) \rightarrow V_C^d$ should have desired transient performance indices. These performance indices should be insensitive to parameter variations of the buck-boost converter and external disturbance represented by varying value of the resistor $R = R(t)$.

In the paper a two-step approach will be used: an inner controller of the current I_L through the inductor with inductance L is designed such that

$$\lim_{t \rightarrow \infty} I_L(t) = I_L^d, \quad (4)$$

and then an outer controller is constructed in order to meet the requirement (3).

3. INNER CONTROLLER DESIGN

3.1 System with continuous control variable

Let x_1 be the measurable output of the system (1)–(2) and consider the system given by

$$\dot{x}_1 = \frac{E}{L}\bar{u} - \frac{x_2}{L}(1-\bar{u}), \quad (5)$$

$$\dot{x}_2 = -\frac{1}{RC}x_2 + \frac{x_1}{C}(1-\bar{u}), \quad (6)$$

where \bar{u} is the continuous control variable. Let $\bar{u} \in (0, 1)$.

First, assume that

$$x_1(t) = r_1 = \text{const}, \quad \forall t \in [0, \infty) \quad (7)$$

where $r_1 = I_L^d$. Then from (5) and (7), we get

$$0 = \frac{E + x_2}{L}\bar{u} - \frac{x_2}{L}. \quad (8)$$

Denote $\bar{u}_{r_1} = \bar{u}(t) \big|_{x_1(t) = r_1}$ as the solution of (8). Hence, we obtain

$$\bar{u}_{r_1} = \frac{x_2}{E + x_2}, \quad x_2 = E \frac{\bar{u}_{r_1}}{1 - \bar{u}_{r_1}}. \quad (9)$$

Since $\bar{u}_{r_1} \in (0, 1)$, we obtain $x_2 \in (0, \infty)$. Then the system (5)–(6), having dimension 2, degenerates into the system

$$\begin{aligned} x_1 &= r_1 = \text{const}, \\ \dot{x}_2 &= -\frac{1}{RC}x_2 + \frac{1}{C} \left[1 - \frac{x_2}{E + x_2} \right] r_1, \end{aligned} \quad (10)$$

having dimension 1. The degenerated system (10) has the unique asymptotically stable positive equilibrium point x_2^s given by

$$x_2^s = \frac{E}{2} \left[\sqrt{1 + \frac{4r_1 R}{E}} - 1 \right]. \quad (11)$$

Therefore, the internal stability of the system (5)–(6) is satisfied under condition that $x_1 = r_1$ (or, in other words, the system (5)–(6) is the minimum phase system).

Second, the variable x_1 is considered as the output of the system (5)–(6). From (5), it follows that the relative degree of this system equals one. Hence, let the desired output behavior of x_1 be assigned by $x_1^{(1)} = F(x_1, r_1)$, where

$$x_1^{(1)} = \frac{1}{T}[r_1 - x_1]. \quad (12)$$

The deviation between the desired dynamics $F(x_1, r_1)$ assigned by (12) and the actual value of the relative highest output derivative $x_1^{(1)}$ is denoted by $e^F = F(x_1, r_1) - x_1^{(1)}$, where e^F is the error of the desired dynamics realization. Then the control problem represented by (4) corresponds to the insensitivity condition given by

$$e^F = 0. \quad (13)$$

Third, the relative degree of the system (5)–(6) equals 1 and its internal stability is satisfied. Therefore, the control law with the 1st output derivative in feedback (Yurkevich, 2004)

$$\mu_1 \bar{u}^{(1)} = k_1 \{T_1^{-1}[r_1 - x_1] - \dot{x}_1^{(1)}\} \quad (14)$$

can be applied in order to meet the requirement (13), where μ_1 is a small positive parameter. Note that (14) corresponds to proportional-integral (PI) controller.

We see that in the closed-loop system given by (5)–(6) and (14), the two-time-scale motions are induced as $\mu_1 \rightarrow 0$. Hence, we obtain the fast-motion subsystem (FMS) given by

$$\mu_1 \bar{u}^{(1)} + k_1 \frac{E + x_2}{L} \bar{u} = k_1 \left\{ \frac{r_1 - x_1}{T_1} + \frac{x_2}{L} \right\}, \quad (15)$$

where x_1, x_2 are the frozen parameters during the transients in (15) and $T_{fms} = \mu_1 L / (E + x_2)$ is the time constant of the fast-motion subsystem. We see that the block diagram of the FMS (15) can be displayed as shown in Fig. 2. We see that the

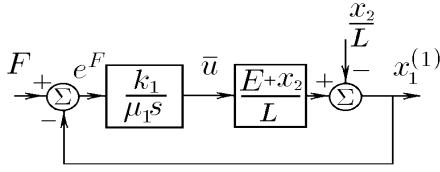


Fig. 2. Block diagram of the FMS in the closed-loop system (5)–(6) controlled by (14).

FMS (15) is stable. Then, letting $\mu \rightarrow 0$ in (15), we obtain the steady state (more precisely, quasi-steady state) of the FMS (15), where $\bar{u}(t) = \bar{u}^s(t)$ and

$$\bar{u}^s = \frac{L}{E + x_2} \left\{ \frac{r_1 - x_1}{T_1} + \frac{x_2}{L} \right\}. \quad (16)$$

Substitution of (16) into (5)–(6) yields the slow-motion subsystem (SMS) given by

$$\dot{x}_1 = \frac{1}{T_1} [r_1 - x_1], \quad (17)$$

$$\dot{x}_2 = -\frac{1}{RC} x_2 + \frac{x_1}{C} \times \left[1 - \frac{L}{E + x_2} \left(\frac{r_1 - x_1}{T_1} + \frac{x_2}{L} \right) \right]. \quad (18)$$

Note that the desired behavior of x_1 in the SMS (17)–(18) is satisfied. By letting $x_1 = r_1$ in (17)–(18), we obtain the degenerated system (10).

Take $E = 15$ V, $L = 0.02$ H, $C = 0.001$ F, $R = 200$ Ω . By linearization of (10) at the equilibrium point x_2^s we obtain $\dot{z} = a_{int} z$ where

$$a_{int} = -\frac{1}{RC} - \frac{2r_1}{C \left[1 + \sqrt{1 + 4r_1 R/E} \right]},$$

and $T_{int} = -1/a_{int}$ is the time constant of the linearized internal subsystem at the point x_2^s .

From the above we get $x_2^s \approx 3.28$ V, $T_{int} \approx 0.03$ s, $T_{fms} \approx 2.2 \cdot 10^{-3}$ s when $r_1 = 0.02$ A. Note that $T_{int} \gg T_{fms}$ where $T_{fms} \rightarrow 0$ as $\mu_1 \rightarrow 0$. Similarly, $x_2^s \approx 48$ V, $T_{int} \approx 0.0036$ s, $T_{fms} \approx 0.63 \cdot 10^{-3}$ s when $r_1 = 1$ A. Note that $T_{int} \gg T_{fms}$ again.

Take $T_1 = 0.02$ s, $\mu_1 = 0.002$ s, and $k_1 = 0.001$ where T_1 and μ_1 are selected such that $T_1 \gg T_{fms}$ and $T_{int} \gg T_{fms}$ to produce slow-fast decomposition in the closed-loop system. Simulation results for the model (5)–(6) controlled by the algorithm (14) are displayed in Fig. 3, where the initial conditions are $x_1(0) = 0.02$ A, $x_2(0) = 3.26$ V, $\bar{u}(0) = 0$, and $t \in [0, 1]$ s. The external disturbance is represented by the varying resistance $R = R(t)$, shown in Fig. 1.

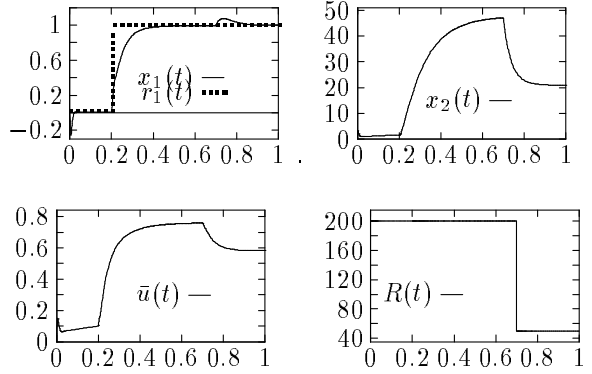


Fig. 3. Simulation results for the system (5)–(6) controlled by (14).

3.2 Switching regulator design

As the next step, let us consider the switching regulator given by

$$\mu_1 u_1^{(1)} = k_1 \{T_1^{-1}[r_1 - x_1] - \dot{x}_1^{(1)}\}, \quad (19)$$

$$u_2(t) = u_1(t - \tau), \quad (20)$$

$$u = \frac{1 + \text{sgn}(u_2)}{2}. \quad (21)$$

Hence, in contrast to Fig. 2, the block diagram of the FMS has modified form, shown in Fig. 4.

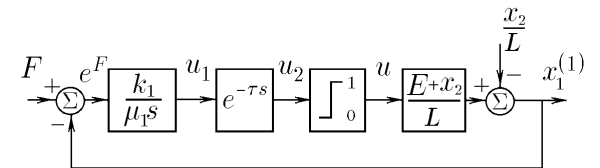


Fig. 4. Block diagram of the FMS in the closed-loop system (1)–(2) controlled by (19)–(21).

The time delay τ is included here in order to satisfy the conditions for limit cycle existence in the

FMS shown in Fig. 4. Assume that the nonlinearity input is $u_2(t)$, where

$$u_2(t) = u_2^0 + A \sin(\omega t)$$

with u_2^0 the constant bias signal. Hence, due to the integral action incorporated in feedback loop, we have

$$\int_t^{t+2\pi/\omega} e^F(\bar{t}) d\bar{t} = 0 \quad (22)$$

for the stationary oscillations in the FMS. So, the average value of e^F corresponds to the insensitivity condition (13) and the desired behavior of $x_1(t)$ with assigned dynamics (12) is satisfied if sufficiently fast oscillations take place. Therefore, the expression (22) represents the insensitivity condition of $x_1(t)$ with respect to external disturbances and variations of parameters of the buck-boost converter in the average sense. We can see that the key element to reach the desirable behavior of $x_1(t)$ is the existence of the fast oscillations in the FMS.

Then, in accordance with the describing function method, let us replace the relay switch by its quasi-linear approximation. Let the integrator $k_1/(\mu_1 s)$ in Fig. 4 displays a low-pass filtering property. Consider the output $u(t)$ of the nonlinearity represented by its Fourier series

$$u(t) = u_0 + \sum_{k=1}^{\infty} \{b_k \sin(k\omega t) + c_k \cos(k\omega t)\} \quad (23)$$

with coefficients u_0, b_k, c_k . Note that the particular feature of the discussed system is the nonsymmetrical limits of the nonlinearity. Hence, $u_2^0 \neq 0$, $u_0 \neq 0$, and it is known that for the given nonlinearity we have (see, e.g., (Paltov, 1975))

$$u_0 = \frac{1}{2} + \frac{1}{\pi} \sin^{-1} \left(\frac{u_2^0}{A} \right), \quad (24)$$

$$b_1 = \frac{2}{\pi} \sqrt{1 - \left[\frac{u_2^0}{A} \right]^2}, \quad (25)$$

$$c_1 = 0, \quad (26)$$

where $A \geq |u_2^0|$ and $y = \sin^{-1}(x)$ denotes the inverse sine of x . Therefore, the sinusoid plus bias describing function of the discussed nonlinear element has the gain for the bias

$$u_0/u_2^0$$

and the gain for the sinusoid

$$G_n(j, A) = \frac{2}{\pi A} \sqrt{1 - \left[\frac{u_2^0}{A} \right]^2}. \quad (27)$$

Assume that $F = 0$. Then, by the block diagram shown in Fig. 4, we get the balance equation for the constant bias signal u_2^0 of the discussed FMS:

$$\left[\frac{1}{2} + \frac{1}{\pi} \sin^{-1} \left(\frac{u_2^0}{A} \right) \right] - \frac{x_2}{E + x_2} = 0. \quad (28)$$

The 1st order harmonic balance equation for the FMS shown in Fig. 4 yields

$$1 - \frac{2(E + x_2)k_1 e^{-j\tau\omega}}{j\mu_1\omega\pi AL} \sqrt{1 - \left[\frac{u_2^0}{A} \right]^2} = 0. \quad (29)$$

From (29) we obtain

$$m^2 A^4 - A^2 + [u_2^0]^2 = 0, \quad (30)$$

$$\omega = \frac{\pi}{2\tau}, \quad (31)$$

where

$$m = \frac{\mu_1 L \pi^2}{4k_1 \tau (E + x_2)}. \quad (32)$$

The oscillations in the FMS induce the oscillations in $x_1(t)$ and have an influence on accuracy of stabilization for $x_1(t)$. Let e_{osc} be the amplitude of the stationary oscillations of $x_1(t)$ with frequency ω . In accordance with Fig. 4, we get to a first approximation

$$e_{osc} \approx \frac{\mu_1}{k_1} A$$

given that ω is sufficiently large. Note that $\omega \rightarrow \infty$ and $A \rightarrow 0$ as $\tau \rightarrow 0$. Hence, $e_{osc} \rightarrow 0$ and an acceptable level of ripple for the output voltage V_{out} can easily be provided by selection of τ .

Take $T_1 = 0.02$ s, $\mu_1 = 0.002$ s, $k_1 = 0.001$, and $\tau = 0.001$ s. From (31) we get $\omega \approx 1570.8$ rad/s. Let $R = 200 \Omega$. The joint numerical resolution of (28) and (30) yields $u_2^0 \approx -0.101$, $A \approx 0.143$, $e_{osc} \approx 0.286$ V when $x_2 = 5$ V, and $u_2^0 \approx 0.327$, $A \approx 0.437$, $e_{osc} \approx 0.874$ V when $x_2 = 50$ V.

Simulation results for the switched system (1)–(2) controlled by the algorithm (19)–(21) are displayed in Fig. 5, where the initial conditions are $x_1(0) = 0.02$ A, $x_2(0) = 3.26$ V, $u_1(0) = 0$ and $R = 200 \Omega$ for all $t \in [0, 0.3]$ s. The simulation results confirm the analytical calculations.

4. OUTER CONTROLLER DESIGN

Let us consider the block diagram of the control system shown in Fig. 6 where the external disturbance is represented by the varying resistance $R = R(t)$ of the buck-boost converter (BBC) and there are two controllers: the designed above inner switching controller C_1 and an outer continuous controller C_2 . Here, we denote $r_2 = V_{out}^d$.

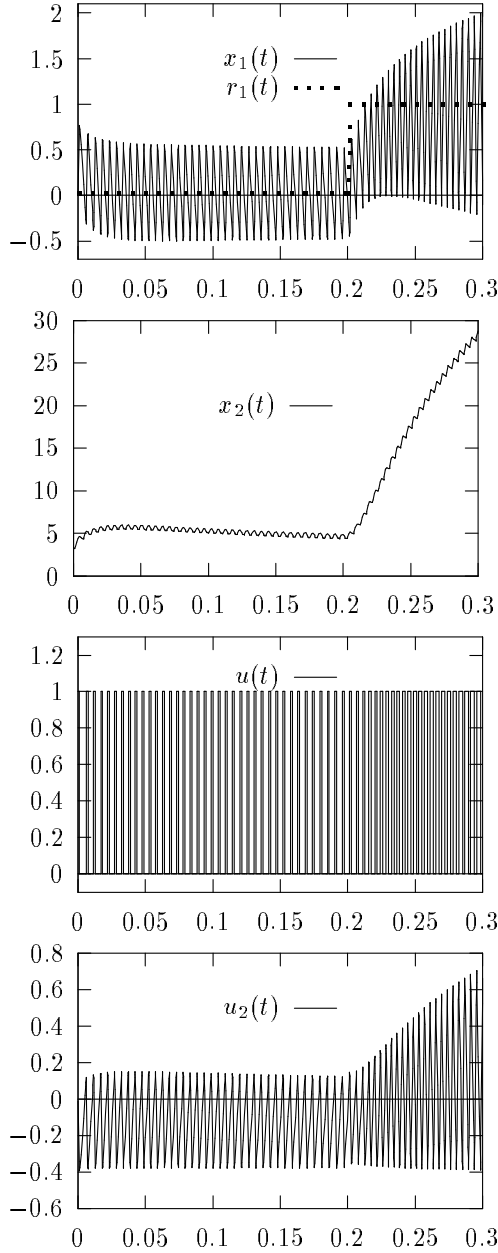


Fig. 5. Simulation results for the switched system (1)–(2) controlled by (19)–(21).

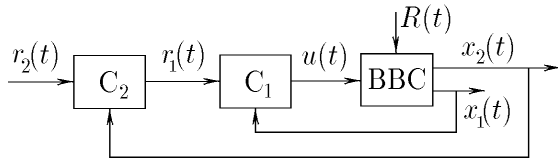


Fig. 6. Block diagram of the closed-loop system with an inner switching controller C_1 and an outer continuous controller C_2 .

Assume that $x_1 = r_1$ in the average sense for the stationary oscillations in the FMS. Then the behavior of $x_2(t)$ can be approximately described by the degenerated system (10) of the 1st order, where r_1 is the new control variable, $x_2(t)$ is the new output variable, and the relative degree of the degenerated system (10) equals 1. Let the desired behavior of x_2 be assigned by

$$x_2^{(1)} = \frac{1}{T_2}[r_2 - x_2]. \quad (33)$$

Therefore, the structure of C_2 can be selected in the form

$$\mu_2 r_1^{(1)} = k_2 \{T_2^{-1}[r_2 - x_2] - x_2^{(1)}\} \quad (34)$$

and designed similar to (14). Hence, from the closed-loop system given by (10), (34), where the two-time-scale motions are induced as $\mu_2 \rightarrow 0$, we obtain the fast-motion subsystem (FMS) given by

$$\mu_2 r_1^{(1)} + \frac{k_2 E}{C(E + x_2)} r_1 = k_2 \left\{ \frac{r_2 - x_2}{T_2} + \frac{k_2 x_2}{C} \right\},$$

where x_2 is the frozen parameter. We get that $\bar{T}_{fms} = \mu_2 C(E + x_2)/(k_2 E)$ is the time constant of this fast-motion subsystem where $\bar{T}_{fms} \in (0.61 \cdot 10^{-2}, 2.1 \cdot 10^{-2})$ when $x_2 \in (3.26, 48)$. The corresponding SMS is the same as (33).

We can take $T_2 = 0.1$ s, $\mu_2 = 0.01$ s, $k_2 = 0.002$ where T_2 and μ_2 are selected such that $T_2 \gg \bar{T}_{fms}$ to produce slow-fast decomposition in the closed-loop system given by (10), (34).

Finally, in order to perform numerical simulation, let us rewrite the inner switching regulator (19)–(21) and the outer controller (34) in the form

$$\begin{aligned} \frac{du_{11}}{dt} &= \frac{k_1}{T_1}[r_1 - x_1], & u_1 &= \frac{1}{\mu_1}[u_{11} - k_1 x_1], \\ u_2(t) &= u_1(t - \tau), & u &= \frac{1 + \text{sgn}(u_2)}{2}, \\ \frac{du_{21}}{dt} &= \frac{k_2}{T_2}[r_2 - x_2], & r_1 &= \frac{1}{\mu_2}[u_{21} - k_2 x_2]. \end{aligned} \quad (35)$$

Simulation results for the switched model (1)–(2) controlled by the algorithm (35) with the assigned above parameters are displayed in Fig. 7 for the time interval $t \in [0, 0.3]$ s, where $r_2 = 49$ V and the initial conditions are the following: $x_1(0) = 1.1$ A, $x_2(0) = 50$ V, $u_{11}(0) = 0$, $u_{21}(0) = 0.11$.

5. CONCLUSIONS

The presented method of switching regulator design allows us to obtain the desired transients for buck-boost converter under uncertainty in model description and in the presence of unknown external disturbances. The discussed control law with the relative highest derivative and small parameter (high gain) in feedback produces slow-fast decomposition in the closed-loop system. It has been shown that if a sufficient time-scale separation between the fast and slow modes and stability of FMS are provided by selection of controller parameters, then SMS equation has the desired form,

and, thus, we have the desired transient performance indices of the current I_L and the voltage V_{out} in the closed-loop system.

REFERENCES

- Bryant, B. and M.K. Kazimierzuk (2002). Derivation of the buck-boost PWM DC-DC converter circuit topology. *Proc. of the IEEE Int. Symp. on Circuits and Systems*, **5**, pp. V-841-V-844.
- Cunha, F. B. and Pagano, D. J. (2002). Limitations in the control of a DC-DC boost converter. *Proc. of 15th IFAC World Congress*, Barcelona, Spain.
- Giral, R., E. Arango, J. Calvente and L. Martinez-Salamero (2002). Inherent DCM operation of the asymmetrical interleaved dual buck-boost. *Proc. of the 28th IEEE Annual Conf. of the Industrial Electronics Society, IECON 02, 5-8 Nov. 2002*, **1**, pp. 129-134.
- Jianping Xu (1991). An analytical technique for the analysis of switching DC-DC converters. *Proc. of the IEEE Int. Symp. on Circuits and Systems*, **2**, pp. 1212-1215.
- Maksimovic, D. and S. Cuk (1991). Switching converters with wide DC conversion range. *IEEE Trans. Power Electronics*, **PE-16**, 1, pp. 151-157.
- Mohan, N., T.M. Undeland and W.P. Robbins (1995). *Power Electronics: Converters, Applications and Design*, Wiley, 802 p.
- Paltov, I.P. (1975). *Transients performance and compensator design for nonlinear control systems*, Nauka, Moscow, 368 p.
- Shtessel, Y.B., A.S.I. Zinober and I.A. Shkolnikov (2002). Boost and buck-boost power converters control via sliding modes using dynamic sliding manifold. *Proc. of the 41st IEEE Conf. on Decision and Control*, **3**, pp. 2456-2461.
- Sira-Ramirez, H. (2002). Sliding modes, passivity, and flatness. In: *Sliding Mode Control in Engineering*, Perruquetti, W. and Barbot, J.P (Eds.), New York: Marcel Dekker, pp. 163-189.
- Suvorov, A. (1991). Synthesis of control systems based on the method of localization of given fast oscillating process. *Proc. of the Int. Workshop on Control System Synthesis: Theory and Application*, (27 May - 1 June, 1991), Novosibirsk, USSR, pp. 93-99.
- Vostrikov, A.S. (1977). On the synthesis of control units of dynamic systems. *Systems Science*, Techn. Univ., Wroclaw, **3**(2), pp. 195-205.
- Yurkevich, V.D. (2004). *Design of nonlinear control systems with the highest derivative in feedback*. (Series on Stability, Vibration and Control of Systems, Series A - Vol.16), World Scientific.

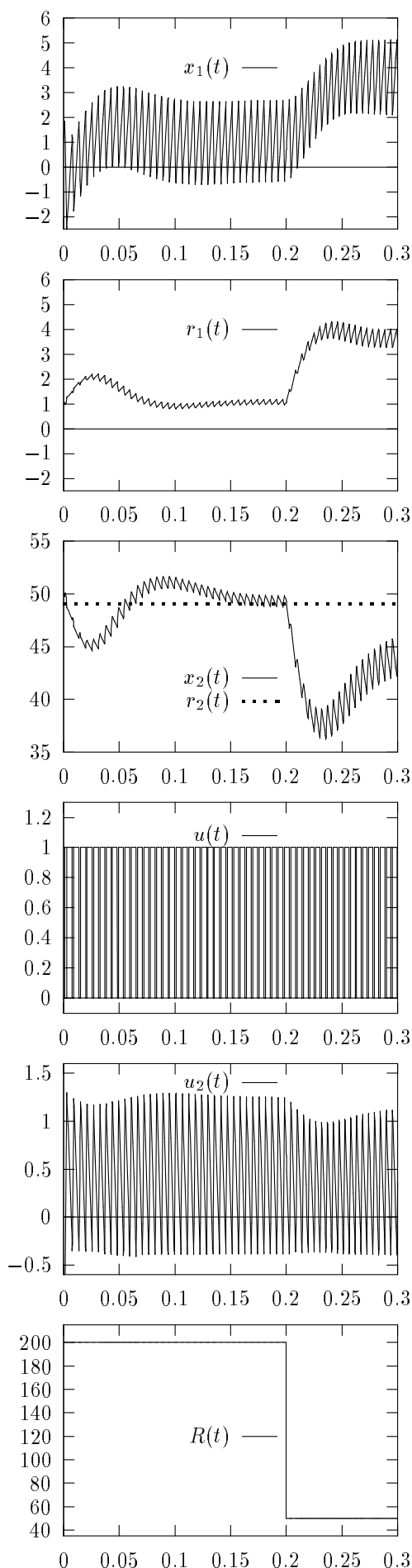


Fig. 7. Simulation results for the switched system (1)–(2) controlled by the algorithm (35).